Hwang Sun Wook (Orcid ID: 0000-0001-8460-7480)

Pamoic Acid-Induced Peripheral GPR35 Activation Improves Pruritus and Dermatitis

Running title

Pamoic acid alleviates itch and dermatitis

Authors

Chaeeun Kim, Yerin Kim, Ji Yeon Lim, Minseok Kim, Haiyan Zheng, Miri Kim, Sun Wook Hwang*

Affiliations

Department of Biomedical Sciences and Department of Physiology, College of Medicine, Korea University, Seoul 02841, Korea.

*Address for correspondence:

Sun Wook Hwang, Ph.D.

Department of Biomedical Sciences, Korea University College of Medicine, Seoul 02841, Korea

This article has been accepted for publication and undergone full peer review but has not been through the copyediting, typesetting, pagination and proofreading process which may lead to differences between this version and the Version of Record. Please cite this article as doi: 10.1111/bph.16201

This article is protected by copyright. All rights reserved.

Tel: +82-2-2286-1204

Fax: +82-2-925-5492

Email address: sunhwang@korea.ac.kr

Abstract

Background and purpose

Pruritic dermatitis is a disease with a considerable unmet need for treatment and appears to present with not only epidermal but also peripheral neuronal complications. Here we propose a novel pharmacologic modulation targeting both peripheral dorsal root ganglion (DRG) sensory neurons and skin keratinocytes. GPR35 is an orphan G-protein-coupled receptor expressed in DRG neurons and has been predicted to downregulate neuronal excitability when activated. Modulator information is currently increasing for GPR35 and pamoic acid (PA), a salt-forming agent for drugs, has been shown to be an activator solely specific for GPR35. Here we investigated its effect on dermatitic pathology.

Experimental Approach

We confirmed GPR35 expression in peripheral neurons and tissues. The effect of PA treatment was pharmacologically evaluated in cultured cells *in vitro* and in *in vivo* animal models for acute and chronic pruritus.

Key results

Local PA application mitigated acute non-histaminergic itch and consistently, obstructed DRG neuronal responses. Keratinocyte fragmentation under dermatitic simulation was also dampened following PA incubation. Chronic pruritus in 1-chloro-2,4-dinitrobenzene (DNCB) and psoriasis models was also moderately but significantly reversed by the repeated

This article is protected by copyright. All rights reserved.

Accepted Article

14765381, ja, Downloaded from https://bpspubs.onlinelibrary.wiley.com/doi/10.1111/bph.16201 by Gachon University Medical, Wiley Online Library on [06/08/2023]. See the Terms and Conditions (https://onlinelibrary.wiley.com/terms-and-conditions) on Wiley Online Library for rules of use; OA articles are governed by the applicable Creative Commons License

applications of PA. Dermatitic scores in the DNCB and psoriatic models were also improved by its application, indicating that it is beneficial for mitigating disease pathology.

Conclusions and Implications

Our findings suggest that pamoic acid activation of peripheral GPR35 can contribute to the improvement of pruritus and its associated diseases.

Key words

Pamoic acid; GPR35; neuron; itch; dermatitis

Bulleted point summary

What is already known

- Peripheral neurons and their molecular components are receiving increasing attention as therapeutic targets for pruritic dermatitis.
- Information on modulators for GPR35, expressed in those neurons, is expanding.

What this study adds

- Treatment with PA, a clinically available GPR35-specific agonist, improved pruritus and dermatitis in animal models.
- Decreased excitabilities of non-histaminergic pruriceptor neurons and prevention of keratinocyte fragmentation may be its critical therapeutic mechanisms.

What is the clinical significance

- We suggest that peripheral GPR35 activation by PA can contribute to the improvement of pruritus and its associated diseases.

This article is protected by copyright. All rights reserved.

Accepted Article

14765381, ja, Downloaded from https://bpspubs.onlinelibrary.wiley.com/doi/10.1111/bph.16201 by Gachon University Medical, Wiley Online Library on [06/08/2023]. See the Terms and Conditions (https://onlinelibrary.wiley.com/terms-and-conditions) on Wiley Online Library for rules of use; OA articles are governed by the applicable Creative Commons License

1. Introduction

Pruritus or itch is a somatic sense that evokes a desire to scratch and is now recognized as a symptom that needs to be controlled in pathologic dermatitis because it is naturally unpleasant, and itch-induced scratch often devastates the skin, particularly under dermatitic condition (Mack and Kim, 2018). Owing to the limitations of antihistamines regarding their tolerance and adverse effects, it is important to secure more diverse therapeutic concepts through proposing new cellular and molecular mechanisms. Since the peripheral dorsal root ganglion (DRG) neurons play a central role as the signal transducer and conductor for itch generation, here we focus on their modulation for relieving itch and related dermatitis (Lee et al., 2018) (Jurcakova et al., 2019).

Among the relatively unexplored molecules present in DRG neurons, we paid attention to those predicted to have pruriceptor-enriched expression and to modulate neuronal function by specific targeting with a clinically available and pharmacologically specific agent. GPR35 is a member of the class A orphan G-protein coupled receptor (GPCR) family with neuronal expression (Ohshiro et al., 2008). Recent expression analysis indicated that C-fibers among DRG neurons are major GPR35 expressers in the nervous system of mice (Zeisel et al., 2018). Signals mediated by GPR35 activation appear to follow the $G\alpha_{i/o}$ pathway, which is considered to downregulate neuronal excitability. (Guo et al., 2008) (Hu et al., 2017). Ionic modulation of nociceptors, which share GRP35 expression with pruriceptors, by GPR35 activation led to analgesia (Resta et al., 2016). Interestingly, pamoic acid (PA), which has been long utilized for the salt formulation of several clinically available drugs, was found to be a GPR35-specific agonist (Zhao et al., 2010). Despite such possibilities to be involved in pruritus and pharmacological modulability, PA nor GPR35 has been under consideration for pruritic modulation. Therefore, here we examine whether PA action on GPR35 may affect

This article is protected by copyright. All rights reserved.

14765381, ja, Downloaded from https://bpspubs.onlinelibrary.wiley.com/doi/10.1111/bph.16201 by Gachon University Medical, Wiley Online Library on [06/08/2023]. See the Terms and Conditions (https://onlinelibrary.wiley.com/terms-and-conditions) on Wiley Online Library for rules of use; OA articles are governed by the applicable Creative Commons License

acute and/or chronic itches or alter dermatitic disease severity.

2. Methods

2.1. Animals

Five to eight-week old male BALB/c mice and six-week-old male ICR mice were purchased from Orient Bio Inc. (Seongnam, Korea) and raised under specific pathogen-free conditions at 24 ± 2℃ and 50 ± 10% humidity with a 12-h light-dark cycle. They were individually housed in ventilated cages and food and water were available *ad libitum*. All animal experiments were approved and conducted in correspondence with the guidelines approved by the institutional animal care and use committee of Korea University (2019-0618).

2.2. Dermatitis models

For observing atopic dermatitis-like chronic pruritus, 2,4-dinitrochlorobenzene (DNCB) was topically applied to BALB/c mice in the nape of their necks. Detailed schedules for the treatment were summarized in Fig. 3. Briefly, six-week-old male BALB/c mice were split into 6 groups: naive control (untreated); control (DNCB and vehicle-treated); DNCB and 1 μM PA-treated; DNCB and 10 μM PA-treated; DNCB and 1 mM PA-treated; DNCB and 30 mM-PA treated. Mice with shaven dorsal hair received DNCB treatment on their dorsal skin according to the experimental plan shown in Fig. 3. To observe psoriatic pruritus, we spread 62.5 mg of 5% imiquimod (IMQ) cream (Aldara™) on the same dorsal site mentioned above daily for seven days. Mice were divided into 5 groups and then tested: treatment with control (IMQ and vehicle); IMQ and 1 μM PA; IMQ and 10 μM PA; IMQ and 1 mM PA; IMQ and 30 mM PA. PA and the relevant vehicles were intradermally applied in the nape skin.

2.3. Measurement of dermatitis score

This article is protected by copyright. All rights reserved.

Accepted Article

14765381, ja, Downloaded from https://bpspubs.onlinelibrary.wiley.com/doi/10.1111/bph.16201 by Gachon University Medical, Wiley Online Library on [06/08/2023]. See the Terms and Conditions (https://onlinelibrary.wiley.com/terms-and-conditions) on Wiley Online Library for rules of use; OA articles are governed by the applicable Creative Commons License

The dorsal skin of mice was digitally photographed to completely cover the entire shaved skin area using a Sony HDR-CX450. The total area of the shaved skin and the lesioned ones showing morphological symptoms such as scaling, erythema, and hemorrhage were demarcated and then their sizes were calculated using ImageJ (version 1.53a). Individual dermatitis scores were defined as the ratio of the quantified lesioned areas compared to the total skin area shaved at each measurement day. The area under the curves were obtained by integrating the ratios over the entire measurement periods and were used to determine trends of the pathologic severity. After hematoxylin and eosin (H&E) staining, the epidermal thickness of the dorsal skin was microscopically observed (BX51-P, Olympus) and measured using ImageJ. In the DNCB model, the scores were collected every other day for 2 weeks. All the quantifications were carried out in a blinded manner.

2.4. Measurement of pruritus score

Mice with shaven dorsal hair went through a four day habituation period in a transparent acrylic box with the same dimensions as experimental housing (4.5 x 4.5 x 7 inches). To inducing acute pruritus, chloroquine (CQ) (200 μg/50 μl) or histamine (Hist) (200 μg/50 μl) or 5-hydroxytryptamine (5-HT) (150 μg/50 μl) or bovine adrenal medulla peptide 8-22 (BAM8-22) (50 nM) was injected intradermally into the shaved nape skin. For the next 30 minutes, scratching bouts with the hind paws were video recorded. Scratching bouts were defined as a series of movements of rubbing or scraping of the nape skin. Scratching of the face, grooming with their front feet, and hind paws movement directed away from the injection site were excluded for this recording (Akiyama et al., 2009). To quantifying pruritus symptoms of DNCB treated animals, we measured the frequencies of hind paw scratching bouts directed towards the agitated dorsal skin for 1 h every other day during the experimental period by observing the recorded video. In IMQ-treated animals, scratching

This article is protected by copyright. All rights reserved.

14765381, ja, Downloaded from https://bpspubs.onlinelibrary.wiley.com/doi/10.1111/bph.16201 by Gachon University Medical, Wiley Online Library on [06/08/2023]. See the Terms and Conditions (https://onlinelibrary.wiley.com/terms-and-conditions) on Wiley Online Library for rules of use; OA articles are governed by the applicable Creative Commons License

frequencies were measured for 1 h every day before IMQ treatment. All the quantifications were carried out in a blinded manner.

2.5. Cheek-assays

Hist (50 μg/10 μl) or CQ (100 μg/10 μl) or 5-HT (100 μg/10 μl) or BAM8-22 (20 μg/10 μl) was injected into the skin of mouse cheek as previously described (Shimada and LaMotte, 2008) (Kardon et al., 2014) (Lu et al., 2018). Briefly, scratching bouts with hindlimb and wiping bouts with forelimb were videotaped and counted for 30 minutes after injection.

2.6. Skin histology, immunohistochemistry, immunocytochemistry, and in situ hybridization

Dorsal skin was sampled from mice under anesthesia with 2% isoflurane and then fixed in 4% paraformaldehyde. Skin samples were embedded in paraffin and sliced into 10-μm-thick sections for hematoxylin and eosin (H&E) staining using a Leica RM2255 microtome (Leica Microsystems). Some of those skin samples were embedded in optimal cutting temperature (OCT) compound and 20-μm-thick section for immunohistochemistry using a Leica CM3050s cryotome. H&E staining was conducted with deparaffinized-skin sections using the Hematoxylin & Eosin Stain Kit (Vector Laboratories). For immunohistochemistry, anti-GPR35 antibody (rabbit, 1:1000, NBP2-24640, Novus; RRID:AB_2941860), anti-PGP9.5 antibody (mouse, 1:2000, ab8189, Abcam; RRID:AB_306343), and anti-transient receptor potential vanilloid subtype 1 (TRPV1) antibody (mouse, 1:100, ab203103, Abcam; RRID:AB_2934112) were used. After stained for 24 h at 4ºC, the sections were stained with secondary antibodies (Alexa 594-labeled {RRID: AB_141633} or Alexa 488-labeled secondary antibodies {RRID: AB_2535792}; Cat# A-21203 and Cat# A-21206, Invitrogen) for 1 h at room temperature and placed under a coverslip, followed by image acquisition with an iRiS Digital imaging system (Logos Biosystems, Anyang, Korea).

This article is protected by copyright. All rights reserved.

14765381, ja, Downloaded from https://bpspubs.onlinelibrary.wiley.com/doi/10.1111/bph.16201 by Gachon University Medical, Wiley Online Library on [06/08/2023]. See the Terms and Conditions (https://onlinelibrary.wiley.com/terms-and-conditions) on Wiley Online Library for rules of use; OA articles are governed by the applicable Creative Commons License

HaCaT keratinocytes (a kind gift from Dr. Ok Sarah Shin at the same institution; RRID:CVCL_0038) were used for immunocytochemistry. Briefly, cultured HaCaT cells were fixated using 4% paraformaldehyde for 15 minutes and permeabilized in 3% donkey serum, 0.3 % Triton X-100 and 1% bovine serum albumin for 1 h at room temperatures. The cells were stained with anti-GPR35 antibody for 24 h at 4ºC, and then incubated with Alexa 488-labeled secondary antibodies for 1 h at room temperatures. The cells were mounted on glass slides with mounting solution containing 4',6-diamidino-2-phenylindole (DAPI), followed by image acquisition with an iRiS Digital imaging system.

In situ hybridization was conducted according to the manufacturer's protocol (Advanced Cell Diagnostics; ACD, Hayward, CA, USA). Briefly, 6-μm-thick dorsal skin were sampled, deparaffinized, and subjected to hybridization with probes specific for Gpr35 mRNA (ACD Cat No. 317411), for mouse peptidylprolyl isomerase B (Ppib) mRNA as a positive control (ACD catalog No. 313911), and for bacterial DapB mRNA as a negative control (ACD catalog No. 310043). Hybridization was visualized with RNAscope 2.5 HD Red Detection Kit (ACD).

2.7. Culture of dorsal root ganglia (DRG) neurons

Cultures were prepared as described previously (Bang et al., 2007) (Bang et al., 2012) (Chiu et al., 2013) (Choi et al., 2019). Briefly, DRG were collected from ICR mice and digested using collagenase type II (Gibco) and Trypsin-EDTA (Thermofisher) in a CO_2 incubator at 37ºC. Cells were dissociated and set on glass coverslips coated with poly-L-ornithine (Sigma-Aldrich) in 24 well cell culture plates filled with complete DMEM medium containing fetal bovine serum, nerve growth factor 2.5S, penicillin, and streptomycin. Cultured cells were

This article is protected by copyright. All rights reserved.

14765381, ja, Downloaded from https://bjspubs.onlinelibrary.wiley.com/doi/10.1111/bph.16201 by Gachon University Medical, Wiley Online Library on [06/08/2023]. See the Terms and Conditions (https://onlinelibrary.wiley.com/terms-and-conditions) on Wiley Online Library for rules of use; OA articles are governed by the applicable Creative Commons License

grown at 37ºC and 5% CO_2 and were used at 24-120 h after culture.

2.8. Intracellular fluorescence Ca^{2+} imaging experiments of cultured cells

The Ca^{2+} fluorescence imaging experiments were carried out as described previously (Bang et al., 2012) (Yoo et al., 2017) (Cho et al., 2021). Briefly, cells were loaded with 5 μM Fura-2 acetoxymethyl ester dye (Invitrogen), 0.02% pluronic F127 (Invitrogen), and Opti-MEM media (Thermo Fisher Scientific) for 40 minutes in a CO_2 incubator. The cells were perfused in 140 mM NaCl, 5 mM KCl, 2 mM $CaCl_2$, 1 mM $MgCl_2$, 10 mM Glucose, and 10 mM HEPES (titrated to pH 7.4 with NaOH) with or without test drugs. Images of dye-loaded cells were obtained with a cooled sCMOS camera (Prime, Teledyne Photometrics, Tucson, Arizona, USA) attached to a microscope (Olympus BX51WI) at a perfusion rate of about 5 ml/minute of test solutions at room temperatures. The ratios of fluorescence intensity at 340 nm and 380 nm wavelengths in each experiment were recorded using SlideBook 6.0 (3i).

2.9. Culture of HaCaT keratinocytes and their dissociation assay

HaCaT keratinocytes were maintained as described previously (Bang et al., 2010a) (Bang et al., 2010b). Briefly, the cells were grown in DMEM containing 10% fetal bovine serum and 1% penicillin/streptomycin at 37ºC and differentiated for five days. Mouse recombinant interleukin-4 (IL-4) (Sigma-Aldrich, St. Louis, MO, USA), interleukin-13 (IL-13) (Sigma-Aldrich), or their vehicle as a negative control was added to the keratinocyte culture medium to reach 10 ng/ml at a final concentration. PA was added to the culture medium to reach 100 nM at a final concentration 1 h prior to the interleukin applications. After 24 h incubation with interleukin or vehicle, Cells were used for the dispase-based keratinocyte dissociation assay. Cells were labeled with carboxyfluorescein succinimidyl ester (CFSE) and washed

This article is protected by copyright. All rights reserved.

14765381, ja, Downloaded from https://bpspubs.onlinelibrary.wiley.com/doi/10.1111/bph.16201 by Gachon University Medical, Wiley Online Library on [06/08/2023]. See the Terms and Conditions (https://onlinelibrary.wiley.com/terms-and-conditions) on Wiley Online Library for rules of use; OA articles are governed by the applicable Creative Commons License

(Omori-Miyake et al., 2014). The cells were then incubated with dispase II (2.4 U/ml) for 30 minutes at 37°C. The dispase solution was carefully removed and 0.5 ml of Hank's Balanced Salt Solution was added. The HaCaT cell layer was pipetted ten times using a 1-ml micropipette. The cell images were obtained in a coded fashion without information on chemical treatment and analyzed under an iRiS Digital imaging system.

2.10. Luciferase Assays

HEK293T cells (RRID:CVCL_0063) tansfected with the mouse Gpr35 (mGpr35) plasmid DNA pRP[Exp]-EGFP/Puro-CAG > mGpr35 [NM_022320.4] (VectorBuilder Inc, Chicago, IL, USA) were used for these assays. We followed the manufacturer's protocol provided for the ONE-Glo™ EX Luciferase Assay System (E8110; Promega, Madison, WI, USA) as described previously (Kim et al., 2022) (Oh et al., 2008). Briefly, the Lipofectamine-vector complex was added to cultured cells seeded in a 96-well plate. For the vector for the luciferase reporter, pGL4.29[luc2P/CRE/Hygro] (Promega) was used. Twenty-four hours after vector complex addition, the luciferase reagent was added to induce the expression of the luciferase gene, and the luminescence was measured by Gen5™ Version 2.0 Data Analysis Software (Bio-Tek Instruments Inc., Winooski, VT, USA).

2.11. Subclustering analysis of single cell RNA-sequencing (scRNA-seq) data

Single cell RNA-sequencing (scRNA-seq) datasets from Gene Expression Omnibus (GEO) accession number GSE139088 were used as raw data. Gene count matrix log-normalization (10,000 scale factor), gene clustering, dimension reduction analysis (UMAP), differential gene expression analysis, and plotting were conducted using R (version 4.1.2) and Seurat (version 4.0.6). The data was imputed for denoising with Markov affinity-based graph imputation of cells (MAGIC, t=8).

This article is protected by copyright. All rights reserved.

Accepted Article

14765381, ja, Downloaded from https://bpspubs.onlinelibrary.wiley.com/doi/10.1111/bph.16201 by Gachon University Medical, Wiley Online Library on [06/08/2023]. See the Terms and Conditions (https://onlinelibrary.wiley.com/terms-and-conditions) on Wiley Online Library for rules of use; OA articles are governed by the applicable Creative Commons License

2.12. Compounds

All the chemicals were purchased from Sigma-Aldrich (St. Louis, MO, USA) unless otherwise described. For intradermal (i.d.) injection, chemicals were dissolved in saline. Topical IMQ cream (5%) for inducing psoriasis was purchased from Dong-A ST (Seoul, Korea). CID 2745687 was purchased from Tocris. CID 2745687 was dissolved in DMSO to be 10 mM for stock. For *in vivo* treatments, PA was diluted in saline (vehicle 1 in Fig. 1) and CID 2745687 was diluted in saline containing 2% tween 80 (vehicle 2 in Fig. 1).

2.13. Statistical analysis

Statistical significance of data was assessed using the two-tailed unpaired Student's t-test (for comparing two groups), one-way analysis of variance (ANOVA) followed by Dunnett's multiple comparison test (for comparing three or more groups), or two-way ANOVA followed by Tukey's post hoc test (comparing daily data from multiple groups) (*** $p<0.001$, ** $p<0.01$, * $p<0.05$). Data are shown as means ± S.E.M.

2.14. Nomenclature of targets and ligands

Key protein targets and ligands in this article are hyperlinked to corresponding entries in http://www.guidetopharmacology.org, and are permanently archived in the Concise Guide to PHARMACOLOGY 2021/22 (Alexander et al., 2021).

3. Results

3.1. GPR35 is expressed in peripheral neurons and epidermis, and PA relieves acute itch.

We tried to determine whether GPR35 is expressed in DRG nerve terminals and conducted

This article is protected by copyright. All rights reserved.

14765381, ja, Downloaded from https://bpspubs.onlinelibrary.wiley.com/doi/10.1111/bph.16201 by Gachon University Medical, Wiley Online Library on [06/08/2023]. See the Terms and Conditions (https://onlinelibrary.wiley.com/terms-and-conditions) on Wiley Online Library for rules of use; OA articles are governed by the applicable Creative Commons License

immunohistochemistry using the skin sections of mice. As a result, TRPV1-positive and bared nerve terminals of non-myelinating C-fibers, which contain both nociceptor and pruriceptor populations were readily stained in GPR35 immunostaining (Fig. 1a). Interestingly, GPR35 was also mildly detected in part of the epidermal regions in this experiment, which is replicated by *in situ* hybridization (Fig. S1). When we reconstructed a Gene Expression Omnibus GSE139088 dataset, which presents subclusters of mouse DRG neuronal populations based on single cell transcriptomics, many GPR35-positive neurons express histamine receptors and non-histaminergic Mas-related G protein coupled receptors (MRGPRs), indicating that GPR35 may be involved in itch sensation (Fig. S2 and S3). Accordingly, we asked whether treatment with PA, the specific GPR35 agonist affects acute pruritic responses (Fig. 1b). When mice were intradermally pretreated with PA in their napes, acute scratches induced by chloroquine (CQ), 5-hydroxytryptamine (5-HT), and bovine adrenal medulla peptide 8-22 (BAM8-22), which are non-histaminergic pruritogens, were significantly reduced (53.5%, 62.4%, and 69.4% reductions) while histamine-induced scratches were not (Fig. 1c-f). The alteration of non-histaminergic itch behaviors by intradermal PA treatment was reproducible in cheek-scratching assays (Fig. 2). To know whether the PA acts in a GPR35-dependent manner, we tried pharmacological antagonism. By conducting an *in vitro* luminescence assay, we confirmed that the human GPR35 antagonist CID 2745687 is also able to antagonize PA-induced activation of murine GPR35 (Fig. S4). The alteration of the non-histaminergic *in vivo* scratching was reversed by concomitant application of CID 2745687, indicating that PA modulates non-histaminergic itches in a GPR35-dependent fashion (Figs. 1 & 2).

3.2. PA treatment alters DRG neuronal responses and keratinocyte dissociation.

To determine whether PA modulation of histaminergic and non-histaminergic components

This article is protected by copyright. All rights reserved.

14765381, ja, Downloaded from https://bpspubs.onlinelibrary.wiley.com/doi/10.1111/bph.16201 by Gachon University Medical, Wiley Online Library on [06/08/2023]. See the Terms and Conditions (https://onlinelibrary.wiley.com/terms-and-conditions) on Wiley Online Library for rules of use; OA articles are governed by the applicable Creative Commons License

occurs on a neuronal scale, we monitored the intracellular Ca^{2+} levels, which reflects neuronal excitations, of primarily cultured DRG neurons (Fig. 3a). Perfusion of 5-HT onto the cultured somatosensory neurons, readily caused intracellular Ca^{2+} increases in some of those neurons (Figs. 3b-c & S5a-c). The Ca^{2+} responses were blunted upon additional PA perfusion and those PA actions were antagonized in the presence of CID 2745687 (Figs. 3d-e & S5b-c). The neuronal Ca^{2+} responses to another non-histaminergic irritant BAM8-22 were also reduced upon PA perfusion, but reduction in histamine-induced responses by PA was less effective (Figs. 3f-j & S5d-i). We also wondered whether GPR35 activation would affect the epidermal components because of their faint expression and observed keratinocyte fragmentation in culture (Omori-Miyake et al., 2014). GPR35 expression was confirmed in the cultured HaCat keratinocytes (Fig. S6a). Incubation of dermatitic interleukins, IL-4 and IL-13 led to significant dissociation of HaCaT keratinocytes, which was reversed by co-incubation of PA (Fig. S6b and c). Therefore, these results suggest that PA-induced GPR35 activation is able to alleviate pruritic neuronal responses mainly in a non-histaminergic population and may also contribute to the maintenance of cellular integrity of keratinocytes during dermatitis-like conditions.

3.3. PA treatment attenuates chronic pruritus.

We further hypothesized PA treatment might contribute to relieving chronic itches and tested this by investigating a 1-chloro-2,4-dinitrobenzene (DNCB)-induced dermatitis model (Fig. 4a). The neuronal and epidermal expression of GPR35 was largely unaltered after inducing dermatitic conditions despite the tendency of increased GPR35-positive axons (Fig. S7). On-site PA injections gave rise to a reduced frequency of spontaneous scratching events targeting the dermatitic nape skin after its second-round treatment when compared to vehicle injection (32.4% at minimal, and 57.9% at maximal significant decreases) (Fig. 4b). The dates of a

This article is protected by copyright. All rights reserved.

14765381, ja, Downloaded from https://bpspubs.onlinelibrary.wiley.com/doi/10.1111/bph.16201 by Gachon University Medical, Wiley Online Library on [06/08/2023]. See the Terms and Conditions (https://onlinelibrary.wiley.com/terms-and-conditions) on Wiley Online Library for rules of use; OA articles are governed by the applicable Creative Commons License

statistically significant reduction that first emerged and the extent of reduction compared to those following vehicle treatment roughly appeared to show dose-dependence. From the twelfth day, PA treatments at all four doses showed statistically significant reductions. DNCB-induced dermatitis is known to more have atopic than psoriatic features. To separately observe psoriatic type of chronic itches, we used a topical imiquimod (IMQ)-spreading model. PA treatment tended to reduce scratching events and the extent of the reductions was also significant, although its dose-dependence was relatively uncertain (Fig. S8). Taken together, these results suggest that PA treatment was effective for attenuating chronic pruritus.

3.4. PA treatment relieves dermatitic symptoms.

Our results illustrating the reductions of both scratches *in vivo* and in keratinocyte fragmentation *in vitro* led to the hypothesis that PA may also improve dermatitic lesions. To determine whether PA treatment did so, we compared multiple different scores reflecting the severity of dermatitis following PA treatment. As a result, erythema and hemorrhage, and scaling were improved particularly upon PA treatment when applied at a higher range of concentrations (Fig. 5). When the scaling parameters and the erythema and hemorrhage parameters were analyzed in a cumulative way for understanding the individual distresses during the entire period, both were improved by 61.2% and 62.9% reductions following 1 mM of PA treatment and by 52.3% and 53.9% reductions following 30 mM of PA treatment. Epidermal thickening also declined upon PA treatment with all ranges of concentrations tested in this study, and the reduction occurred in a dose-dependent manner (Fig. 6). Since the effect of PA *in vivo* appeared to be roughly saturated at 1 mM for multiple types of scores when compared to those at 30 mM, millimolar or slightly lower concentrations seem to be optimal for this improvement and other non-specific mechanisms at higher doses seem to be less feasible. Mildly improved dermatitic morphology by PA was also observed in the IMQ-

This article is protected by copyright. All rights reserved.

14765381, ja, Downloaded from https://bpspubs.onlinelibrary.wiley.com/doi/10.1111/bph.16201 by Gachon University Medical, Wiley Online Library on [06/08/2023]. See the Terms and Conditions (https://onlinelibrary.wiley.com/terms-and-conditions) on Wiley Online Library for rules of use; OA articles are governed by the applicable Creative Commons License

spreading psoriatic model in a similar dose-dependent tendency (Fig S8c). Overall, these results suggest that PA seems to suppress acute and dermatitic pruritus likely via peripheral GPR35 activation, in turn, this mechanism may also contribute to the improvement of dermatitic lesions.

4. Discussion

Pruritus is now recognized as a deleterious sensation with a negative impact on the quality of life of those affected, particularly in various cases of pathologic skin diseases. Controlling pruritus also seems to be crucial for treating such diseases because pruritic scratches on the lesions frequently interfere with its improvement by disrupting the skin barrier and facilitating infection. Furthermore, this may lead to a vicious cycle called the itch-scratch cycle, often deteriorating their pathologic status (Mack and Kim, 2018). Despite such importance, clinically available therapeutic treatments, mainly based on antihistamine mechanisms, have limited efficacies in relieving itch. Therefore, preparations of other multiple proofs of concepts based on novel different mechanisms are required. Here we focused on targeting a receptor molecule recently shown to have expressions in pruritus-related neurons and to relax their excitability when activated (Ohshiro et al., 2008).

PA has been used as a salt-forming agent which enhances the solubilities of basic chemicals through hydrogen bonding. Surprisingly, PA has been shown to specifically activate GPR35 (Zhao et al., 2010) (Zhao et al., 2014). In our study, because the receptor activation causes $G\alpha_{i/o}$-coupled relaxation of sensory neuronal excitability, we hypothesized that it might reduce itch sensation, subsequently benefitting the improvement of disease itself. As a result, PA treatment suppressed scratching behaviors in both acute and chronic pruritus and even moderately improved disease scores in the DNCB-provoked dermatitis model. By and large,

This article is protected by copyright. All rights reserved.

14765381, ja, Downloaded from https://bpspubs.onlinelibrary.wiley.com/doi/10.1111/bph.16201 by Gachon University Medical, Wiley Online Library on [06/08/2023]. See the Terms and Conditions (https://onlinelibrary.wiley.com/terms-and-conditions) on Wiley Online Library for rules of use; OA articles are governed by the applicable Creative Commons License

our localized applications of PA were effective at relatively high concentrations, which seems to reflect the previously reported potencies of PA on GPR35 (Alexander et al., 2021, Hu et al., 2017, Sharmin et al., 2020, Zhao et al., 2010). Therefore, the topical application of PA might practically work better than systemic application, but this remains to be clarified in the further preclinical studies. Interestingly, clinically available antihistamines such as hydroxyzine are known to be formulated with PA to promoting their water solubility for systemic absorption. Because the dosage of PA in such medication is far lower than necessary to reach the effective window for GPR35 activation in a localized area, such drugs are unlikely to exert off-target effects through actions on GPR35-positive nerves in localized sites of injury.

PA treatment more effectively altered non-histaminergic acute responses than histaminergic ones. This suggests that PA-induced and GRP35-mediated mechanisms may better operate in pruriceptor neuronal subpopulations where non-histaminergic molecular machinery is active. However, this result does not appear to be completely consistent with previous reports conducting massive expression analyses using somatosensory neurons. GPR35 expression has been shown to have relatively broad distribution profiles in non-peptidergic neuronal populations covering both histamine receptor-positive and -negative neurons including neurons expressing metabotropic 5-HT_1 and 5-HT_4 receptor subtypes or Mas-related GPCR series (Usoskin et al., 2015) (Zeisel et al., 2018) (Renthal et al., 2020). Such broad co-expressions are reproducible in our reconstruction analysis for subclustering DRG neurons using GSE139088 dataset (Sharma et al., 2020). Rather than co-expression profiles being simply important, it is possible that a specific merge of paralleled intracellular signals, in this case, GPR35-mediated and non-histaminergic processes, may be more critical, thus mainly affecting non-histaminergic pruritus, but this awaits a future signaling cascade study.

This article is protected by copyright. All rights reserved.

14765381, ja, Downloaded from https://bpspubs.onlinelibrary.wiley.com/doi/10.1111/bph.16201 by Gachon University Medical, Wiley Online Library on [06/08/2023]. See the Terms and Conditions (https://onlinelibrary.wiley.com/terms-and-conditions) on Wiley Online Library for rules of use; OA articles are governed by the applicable Creative Commons License

As mentioned above, the sensory neuronal expression of GPR35 is apparent. The Linnarson lab has demonstrated that among neurons and non-neuronal cells in the central and peripheral nervous systems of mice, GPR35 is expressed almost exclusively in C-fiber DRG neurons, very probably including both pruriceptors and nociceptors (Zeisel et al., 2018). Obviously, GPR35 has been recently reported to exert anti-nociceptive effects (Cosi et al., 2011) (Rojewska et al., 2018) (Rojewska et al., 2019). Regarding the neuronal populations that express GPR35, not only pain but also itch may be strongly affected by GPR35 modulation, the latter of which we first demonstrated here. Genetic associations between a human GPR35 variant and five different chronic inflammatory diseases were once raised and interestingly, one of the associations was with psoriasis (Ellinghaus et al., 2016). Because increased DRG neuronal excitability caused by an aberrant receptor function may exacerbate tissue inflammation, which is called neurogenic inflammation, psoriasis may be hypothesized to led by GPR35 dysfunction, and here we experimentally detected a significant difference in psoriatic itch following PA treatment. Both in our DNCB and IMQ dermatitis models, maximal improvement in multiple parameters by PA commonly appeared to be 50% or so in quantification analyses. Possibly, as an adaptive mechanism, unknown endogenous ligands for GPR35 might already be saturated. Otherwise, other GPR35 expressers, in a remote time and place in which PA was injected in this study, might be also important since, besides the nervous system, some immune components are shown to express GPR35 (Quon et al., 2020) (Sharmin et al., 2020) (Wang et al., 2006). In expression profiling in our hands using mouse skin sections, however, there was no significant detection in disease-infiltrated components. Further studies with an immunological perspective need to delve into this influence.

Although a recent study on the expression profiling using skin single-cell RNAs suggested

This article is protected by copyright. All rights reserved.

14765381, ja, Downloaded from https://bpspubs.onlinelibrary.wiley.com/doi/10.1111/bph.16201 by Gachon University Medical, Wiley Online Library on [06/08/2023]. See the Terms and Conditions (https://onlinelibrary.wiley.com/terms-and-conditions) on Wiley Online Library for rules of use; OA articles are governed by the applicable Creative Commons License

that the presence of GPR35 was uncertain (Haensel et al., 2020), GRP35 expression in intestinal cells of epithelial origin has been previously reproduced (Wang et al., 2006) (Guo et al., 2017) (Tsukahara et al., 2017). In our study, mild immunoreactivity and mRNA signals were detected in the epidermis and PA treatment could alter keratinocyte morphology. Changes in cellular integrity upon PA treatment indicate that PA may more or less contribute to the maintenance of epidermal barrier function and the prevention of scaling. Therefore, it would be further explorable that GPR35-mediated intracellular signaling, different from neuronal one by which this GPR may be engaged in the excitability, may affect the expression or reorganization of keratins and desmosomal components as shown to be vulnerable to the exposure of dermatitic cytokines in a previous study (Omori-Miyake et al., 2014). Collectively, neuronal and epidermal activation of GPR35 both seem to be beneficial for improving skin lesions.

Here we sought to find a novel proof of concept for obstructing pruritus and scratching and thus suggest localized PA treatment underpinned by neuronal GPR35 activation for such a purpose. Also helping keratinocytes maintain their integrity, PA further seems to contribute to mitigation of dermatitis. Because PA is an ingredient that has already been clinically utilized, it may hold a new potential for alleviating pruritic diseases. As well, future discoveries looking for more specific and potent GPR35 activators will be valuable to better modulate sensory diseases involving DRG neurons.

Conflict of interest

The authors have no conflict of interest regarding the publication of this article.

This article is protected by copyright. All rights reserved.

Accepted Article

14765381, ja, Downloaded from https://bpspubs.onlinelibrary.wiley.com/doi/10.1111/bph.16201 by Gachon University Medical, Wiley Online Library on [06/08/2023]. See the Terms and Conditions (https://onlinelibrary.wiley.com/terms-and-conditions) on Wiley Online Library for rules of use; OA articles are governed by the applicable Creative Commons License

Data Availability Statement

Data in this study are available from the corresponding author upon request.

Author contributions

Conceptualization, C.K., S.W.H.; Data curation, C.K. Y.K., J.Y.L.; Funding acquisition, S.W.H.; Investigation, C.K., M.K.; Methodology, C.K., J.Y.L., Y.K., M.K., H.Z.; Supervision, S.W.H.; Writing – original draft, C.K., S.W.H.; Writing – review & editing, C.K., S.W.H.

Declaration of transparency and scientific rigour

This Declaration acknowledges that this paper adheres to the principles for transparent reporting and scientific rigour of preclinical research as stated in the BJP guidelines for Design and Analysis, Immunoblotting and Immunochemistry, and Animal Experimentation, and as recommended by funding agencies, publishers and other organizations engaged with supporting research.

Acknowledgement

This work was supported by grants from the National Research Foundation of Korea (2022M3E5E8081190 and 2022R1A4A2000827). Dr. Woong Sun provided valuable comments on image analysis.

References

Akiyama T, Merrill AW, Zanotto K, Carstens MI, Carstens E. Scratching behavior and Fos expression in superficial dorsal horn elicited by protease-activated receptor agonists and other itch mediators in mice. J Pharmacol Exp Ther 2009;329(3):945-51.

Alexander SP, Kelly E, Mathie A, Peters JA, Veale EL, Armstrong JF et al. The Concise Guide to PHARMACOLOGY 2021/22. Br J Pharmacol 2021;178(S1):S1-S513.

Bang S, Kim KY, Yoo S, Lee SH, Hwang SW. Transient receptor potential V2 expressed in

This article is protected by copyright. All rights reserved.

14765381, ja, Downloaded from https://bpspubs.onlinelibrary.wiley.com/doi/10.1111/bph.16201 by Gachon University Medical, Wiley Online Library on [06/08/2023]. See the Terms and Conditions (https://onlinelibrary.wiley.com/terms-and-conditions) on Wiley Online Library for rules of use; OA articles are governed by the applicable Creative Commons License

sensory neurons is activated by probenecid. Neurosci Lett 2007;425(2):120-5.
Bang S, Yoo S, Yang TJ, Cho H, Hwang SW. Farnesyl pyrophosphate is a novel pain-producing molecule via specific activation of TRPV3. J Biol Chem 2010a;285(25):19362-71.
Bang S, Yoo S, Yang TJ, Cho H, Hwang SW. 17(R)-resolvin D1 specifically inhibits transient receptor potential ion channel vanilloid 3 leading to peripheral antinociception. Br J Pharmacol 2012;165(3):683-92.
Bang S, Yoo S, Yang TJ, Cho H, Kim YG, Hwang SW. Resolvin D1 attenuates activation of sensory transient receptor potential channels leading to multiple anti-nociception. Br J Pharmacol 2010b;161(3):707-20.
Chiu IM, Heesters BA, Ghasemlou N, Von Hehn CA, Zhao F, Tran J, et al. Bacteria activate sensory neurons that modulate pain and inflammation. Nature 2013;501(7465):52-7.
Cho PS, Lee HK, Choi YI, Choi SI, Lim JY, Kim M, et al. GPR171 Activation Modulates Nociceptor Functions, Alleviating Pathologic Pain. Biomedicines 2021;9(3).
Choi G, Yang TJ, Yoo S, Choi SI, Lim JY, Cho PS, et al. TRPV4-Mediated Anti-nociceptive Effect of Suberanilohydroxamic Acid on Mechanical Pain. Mol Neurobiol 2019;56(1):444-53.
Cosi C, Mannaioni G, Cozzi A, Carla V, Sili M, Cavone L, et al. G-protein coupled receptor 35 (GPR35) activation and inflammatory pain: Studies on the antinociceptive effects of kynurenic acid and zaprinast. Neuropharmacology 2011;60(7-8):1227-31.
Divorty N, Jenkins L, Ganguly A, Butcher AJ, Hudson BD, Schulz S et al. Agonist-induced phosphorylation of orthologues of the orphan receptor GPR35 functions as an activation sensor. J Biol Chem 2022;298(3):101655.
Ellinghaus D, Jostins L, Spain SL, Cortes A, Bethune J, Han B, et al. Analysis of five chronic inflammatory diseases identifies 27 new associations and highlights disease-specific patterns at shared loci. Nat Genet 2016;48(5):510-8.
Guo J, Williams DJ, Puhl HL, 3rd, Ikeda SR. Inhibition of N-type calcium channels by activation of GPR35, an orphan receptor, heterologously expressed in rat sympathetic neurons. J Pharmacol Exp Ther 2008;324(1):342-51.
Guo YJ, Zhou YJ, Yang XL, Shao ZM, Ou ZL. The role and clinical significance of the CXCL17-CXCR8 (GPR35) axis in breast cancer. Biochem Biophys Res Commun 2017;493(3):1159-67.
Haensel D, Jin S, Sun P, Cinco R, Dragan M, Nguyen Q, et al. Defining Epidermal Basal Cell States during Skin Homeostasis and Wound Healing Using Single-Cell Transcriptomics. Cell Rep 2020;30(11):3932-47 e6.
Hu HH, Deng H, Ling S, Sun H, Kenakin T, Liang X, et al. Chemical genomic analysis of GPR35 signaling. Integr Biol (Camb) 2017;9(5):451-63.
Jurcakova D, Ru F, Undem BJ. Allergen-induced histaminergic and non-histaminergic activation of itch C-fiber nerve terminals in mouse skin. Neuroscience 2019;410:55-8.
Kardon AP, Polgar E, Hachisuka J, Snyder LM, Cameron D, Savage S, et al. Dynorphin acts as a neuromodulator to inhibit itch in the dorsal horn of the spinal cord. Neuron 2014;82(3):573-86.
Kim Y, Kim C, Lee H, Kim M, Zheng H, Lim JY, et al. Gpr83 tunes nociceptor function, controlling pain. Neurotherapeutics 2022; doi: 10.1007/s13311-022-01327-3. Online

This article is protected by copyright. All rights reserved.

14765381, ja, Downloaded from https://bpspubs.onlinelibrary.wiley.com/doi/10.1111/bph.16201 by Gachon University Medical, Wiley Online Library on [06/08/2023]. See the Terms and Conditions (https://onlinelibrary.wiley.com/terms-and-conditions) on Wiley Online Library for rules of use; OA articles are governed by the applicable Creative Commons License

ahead of print.
Lee SH, Cho PS, Tonello R, Lee HK, Jang JH, Park GY, et al. Peripheral serotonin receptor 2B and transient receptor potential channel 4 mediate pruritus to serotonergic antidepressants in mice. J Allergy Clin Immunol 2018;142(4):1349-52 e16.
Lu YC, Wang YJ, Lu B, Chen M, Zheng P, Liu JG. ACC to Dorsal Medial Striatum Inputs Modulate Histaminergic Itch Sensation. J Neurosci 2018;38(15):3823-39.
Mack MR, Kim BS. The Itch-Scratch Cycle: A Neuroimmune Perspective. Trends Immunol 2018;39(12):980-91.
Oh DY, Yoon JM, Moon MJ, Hwang JI, Choe H, Lee JY, et al. Identification of farnesyl pyrophosphate and N-arachidonylglycine as endogenous ligands for GPR92. J Biol Chem 2008;283(30):21054-64.
Ohshiro H, Tonai-Kachi H, Ichikawa K. GPR35 is a functional receptor in rat dorsal root ganglion neurons. Biochem Biophys Res Commun 2008;365(2):344-8.
Omori-Miyake M, Yamashita M, Tsunemi Y, Kawashima M, Yagi J. In vitro assessment of IL-4- or IL-13-mediated changes in the structural components of keratinocytes in mice and humans. J Invest Dermatol 2014;134(5):1342-50.
Quon T, Lin LC, Ganguly A, Tobin AB, Milligan G. Therapeutic Opportunities and Challenges in Targeting the Orphan G Protein-Coupled Receptor GPR35. ACS Pharmacol Transl Sci 2020;3(5):801-12.
Renthal W, Tochitsky I, Yang L, Cheng YC, Li E, Kawaguchi R, et al. Transcriptional Reprogramming of Distinct Peripheral Sensory Neuron Subtypes after Axonal Injury. Neuron 2020;108(1):128-44 e9.
Resta F, Masi A, Sili M, Laurino A, Moroni F, Mannaioni G. Kynurenic acid and zaprinast induce analgesia by modulating HCN channels through GPR35 activation. Neuropharmacology 2016;108:136-43.
Rojewska E, Ciapala K, Mika J. Kynurenic acid and zaprinast diminished CXCL17-evoked pain-related behaviour and enhanced morphine analgesia in a mouse neuropathic pain model. Pharmacol Rep 2019;71(1):139-48.
Rojewska E, Piotrowska A, Jurga A, Makuch W, Mika J. Zaprinast diminished pain and enhanced opioid analgesia in a rat neuropathic pain model. Eur J Pharmacol 2018;839:21-32.
Sharmin O, Abir AH, Potol A, Alam M, Banik J, Rahman A, et al. Activation of GPR35 protects against cerebral ischemia by recruiting monocyte-derived macrophages. Sci Rep 2020;10(1):9400.
Shimada SG, LaMotte RH. Behavioral differentiation between itch and pain in mouse. Pain 2008;139(3):681-7.
Tsukahara T, Hamouda N, Utsumi D, Matsumoto K, Amagase K, Kato S. G protein-coupled receptor 35 contributes to mucosal repair in mice via migration of colonic epithelial cells. Pharmacol Res 2017;123:27-39.
Usoskin D, Furlan A, Islam S, Abdo H, Lonnerberg P, Lou D, et al. Unbiased classification of sensory neuron types by large-scale single-cell RNA sequencing. Nat Neurosci 2015;18(1):145-53.
Wang J, Simonavicius N, Wu X, Swaminath G, Reagan J, Tian H, et al. Kynurenic acid as a

This article is protected by copyright. All rights reserved.

14765381, ja, Downloaded from https://bpspubs.onlinelibrary.wiley.com/doi/10.1111/bph.16201 by Gachon University Medical, Wiley Online Library on [06/08/2023]. See the Terms and Conditions (https://onlinelibrary.wiley.com/terms-and-conditions) on Wiley Online Library for rules of use; OA articles are governed by the applicable Creative Commons License

ligand for orphan G protein-coupled receptor GPR35. J Biol Chem 2006;281(31):22021-8.

Yoo S, Choi SI, Lee S, Song J, Yang C, Bang S, et al. Endogenous TRPV4 Expression of a Hybrid Neuronal Cell Line N18D3 and Its Utilization to Find a Novel Synthetic Ligand. J Mol Neurosci 2017;63(3-4):422-30.

Zeisel A, Hochgerner H, Lonnerberg P, Johnsson A, Memic F, van der Zwan J, et al. Molecular Architecture of the Mouse Nervous System. Cell 2018;174(4):999-1014 e22.

Zhao P, Lane TR, Gao HG, Hurst DP, Kotsikorou E, Le L, et al. Crucial positively charged residues for ligand activation of the GPR35 receptor. J Biol Chem 2014;289(6):3625-38.

Zhao P, Sharir H, Kapur A, Cowan A, Geller EB, Adler MW, et al. Targeting of the orphan receptor GPR35 by pamoic acid: a potent activator of extracellular signal-regulated kinase and beta-arrestin2 with antinociceptive activity. Mol Pharmacol 2010;78(4):560-8.

Accepted Article

This article is protected by copyright. All rights reserved.

14765381, ja, Downloaded from https://bsppubs.onlinelibrary.wiley.com/doi/10.1111/bph.16201 by Gachon University Medical, Wiley Online Library on [06/08/2023]. See the Terms and Conditions (https://onlinelibrary.wiley.com/terms-and-conditions) on Wiley Online Library for rules of use; OA articles are governed by the applicable Creative Commons License

Figure 1

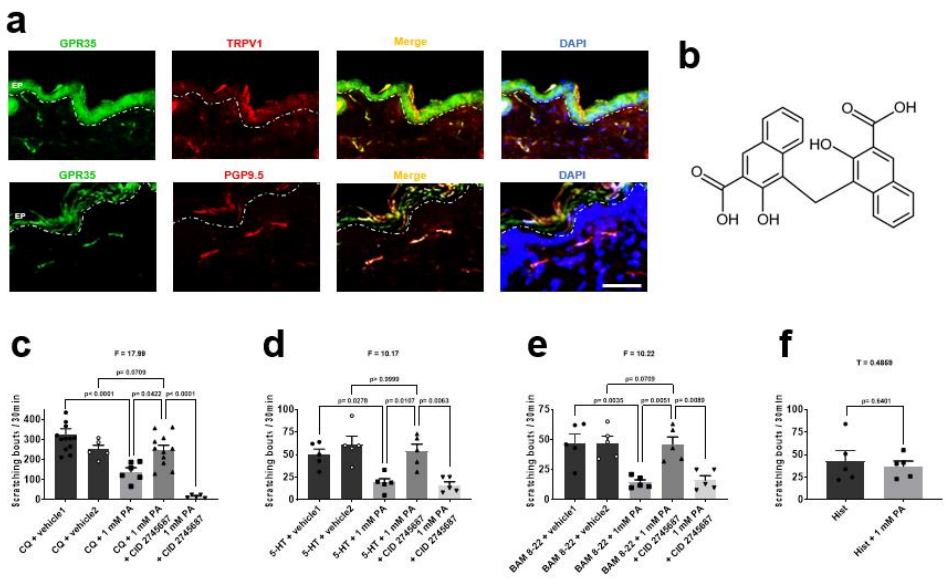

Figure 1. GPR35 expression in nerve terminals and skin and the effects of peripheral treatment of pamoic acid (PA), a GPR35 agonist, on acute itches.

(a) Representative images of immunofluorescent staining with antibodies against GPR35 and TRPV1 (upper panel) or PGP9.5 (lower panel) in the vertical sections of the dorsal skin of mice (scale bar, 50 μm). **(b)** Chemical structure of PA. **(c-e)** PA treatment suppressed non-histaminergic itches. Intradermally injected chloroquine (CQ) (*c*), 5-hydroxytryptamine (5-HT) (*d*), and BAM8-22 (*e*)-provoked scratching behaviors, which were significantly attenuated when PA pretreated 30 minutes prior to observation. Concomitant pretreatment with CID 2745687, a human GPR35 antagonist, significantly antagonized the PA effect (n = 5-12 per group). Pretreatment of CID 2745687 alone did not induce scratches or significantly alter the CQ-induced scratches in the observation period (data not shown). **(f)** Intradermally injected histamine (Hist)-provoked scratching behaviors, which were statistically tolerant to 50 μl intradermal pretreatment of 1 mM PA (n = 5 per group).

This article is protected by copyright. All rights reserved.

14765381, ja, Downloaded from https://bpspubs.onlinelibrary.wiley.com/doi/10.1111/bph.16201 by Gachon University Medical, Wiley Online Library on [06/08/2023]. See the Terms and Conditions (https://onlinelibrary.wiley.com/terms-and-conditions) on Wiley Online Library for rules of use; OA articles are governed by the applicable Creative Commons License

Figure 2

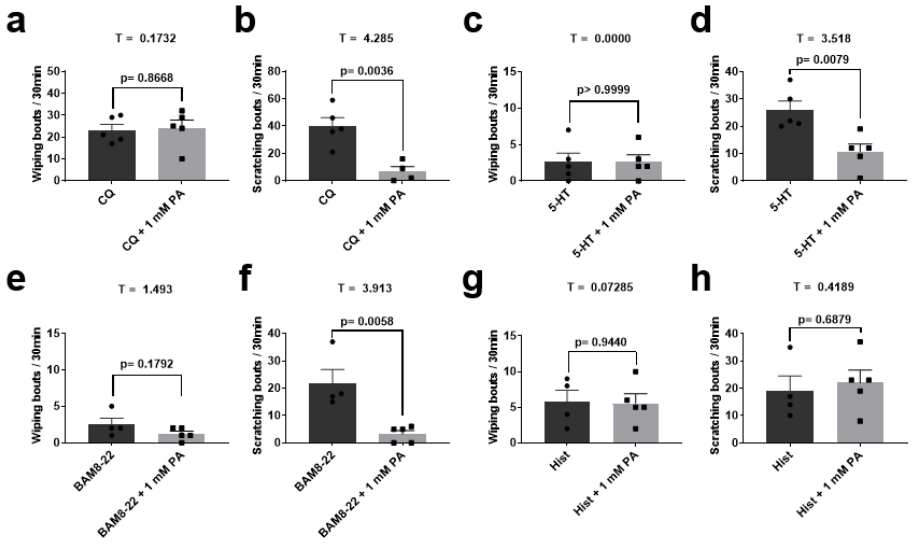

Figure 2. The effects of peripheral treatment of PA in Cheek-assays.

(a-b) Wiping (*a*) nocifensive behaviors and scratching pruritic behaviors (*b*) were quantified for mice with intradermal CQ injection into their cheeks. **(c-d)** Same behaviors as in (*a-b*) were quantified for mice with intradermal 5-HT injection into their cheeks. **(e-f)** Same behaviors as in (*a-b*) were quantified for mice with intradermal BAM8-22 injection into their cheeks. **(g-h)** Same behaviors as in (*a-b*) were quantified for mice with intradermal Hist injection into their cheeks. CQ, 5-HT, and BAM8-22-induced cheek scratching was significantly reduced by intradermal pretreatment of 1 mM PA (*b, d, and f*).

This article is protected by copyright. All rights reserved.

14765381, ja, Downloaded from https://bpspubs.onlinelibrary.wiley.com/doi/10.1111/bph.16201 by Gachon University Medical, Wiley Online Library on [06/08/2023]. See the Terms and Conditions (https://onlinelibrary.wiley.com/terms-and-conditions) on Wiley Online Library for rules of use; OA articles are governed by the applicable Creative Commons License

Figure 3

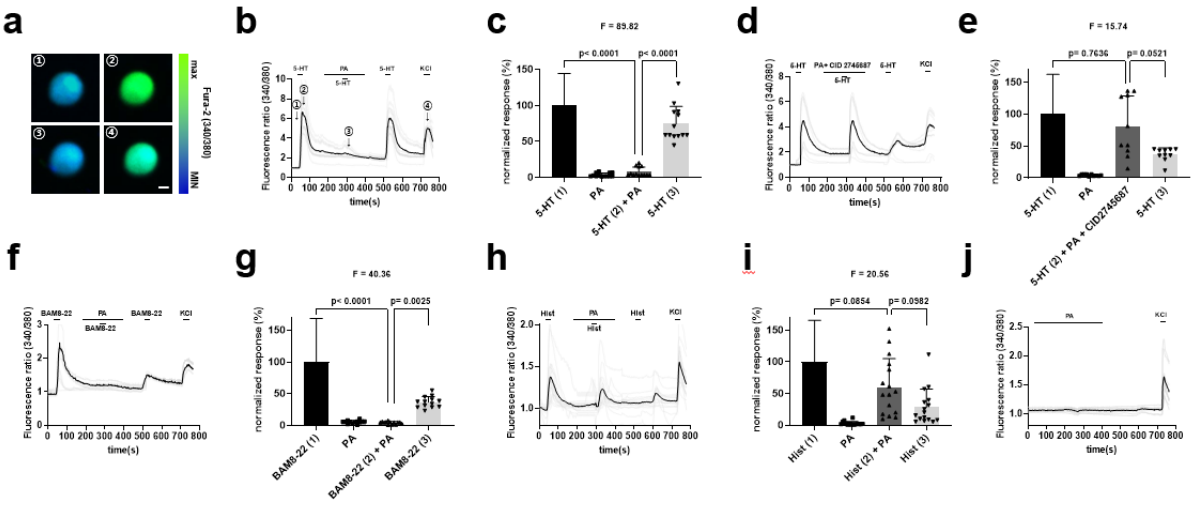

Figure 3. PA treatment suppressed pruritogen-provoked responses in cultured dorsal root ganglion (DRG) neurons.

(a) Intracellular Ca^{2+} fluorescence of neurons was monitored using Fura-2 imaging. Four pseudo-color cell images represent the fluorescence level at the time points indicated in the black trace of the graph (*b*). **(b)** Intracellular Ca^{2+} increases in DRG neurons upon 100 μM 5-HT application were blunted by 100 nM PA treatment. Ca^{2+} traces of the individual cells (grey lines) and the representative to the mean level (black line) are shown. **(c)** The averages of peak intracellular Ca^{2+} increases in DRG neurons upon 5-HT application with or without PA treatment shown in *(b)* were summarized in the histogram (n = 13). **(d)** Intracellular Ca^{2+} increases in DRG neurons upon 100 μM 5-HT application were not significantly affected by 100 nM PA treatment in the presence of 10 μM CID 2745687. **(e)** The averages of peak intracellular Ca^{2+} increases in DRG neurons upon 5-HT application with or without PA and CID 2745687 treatment shown in *(d)* were summarized in the histogram (n = 10). **(f)** Intracellular Ca^{2+} increases in DRG neurons upon 2 μM BAM8-22 application were blunted

This article is protected by copyright. All rights reserved.

14765381, ja, Downloaded from https://bsppubs.onlinelibrary.wiley.com/doi/10.1111/bph.16201 by Gachon University Medical, Wiley Online Library on [06/08/2023]. See the Terms and Conditions (https://onlinelibrary.wiley.com/terms-and-conditions) on Wiley Online Library for rules of use; OA articles are governed by the applicable Creative Commons License

by 100 nM PA treatment. **(g)** The averages of peak intracellular Ca^{2+} increases in DRG neurons upon BAM8-22 application with or without PA treatment shown in *(f)* were summarized in the histogram (n = 13). **(h)** Intracellular Ca^{2+} increases in DRG neurons upon 100 μM histamine (Hist) application were not significantly affected by 100 nM PA treatment. **(i)** The averages of peak intracellular Ca^{2+} increases in DRG neurons upon Hist application with or without PA treatment shown in *(h)* were summarized in the histogram (n = 16). **(j)** Intracellular Ca^{2+} levels in DRG neurons were unaffected upon PA application (n=11).

Accepted Article

This article is protected by copyright. All rights reserved.

14765381, ja, Downloaded from https://bjspubs.onlinelibrary.wiley.com/doi/10.1111/bph.16201 by Gachon University Medical, Wiley Online Library on [06/08/2023]. See the Terms and Conditions (https://onlinelibrary.wiley.com/terms-and-conditions) on Wiley Online Library for rules of use; OA articles are governed by the applicable Creative Commons License

Figure 4

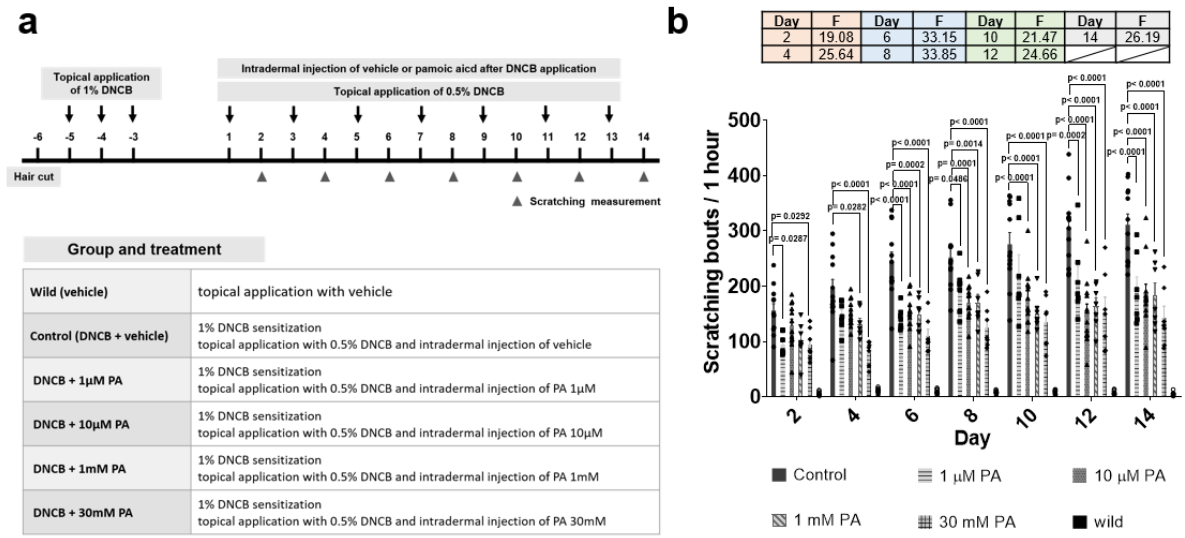

Group and treatment	
Wild (vehicle)	topical application with vehicle
Control (DNCB + vehicle)	1% DNCB sensitization topical application with 0.5% DNCB and intradermal injection of vehicle
DNCB + 1μM PA	1% DNCB sensitization topical application with 0.5% DNCB and intradermal injection of PA 1μM
DNCB + 10μM PA	1% DNCB sensitization topical application with 0.5% DNCB and intradermal injection of PA 10μM
DNCB + 1mM PA	1% DNCB sensitization topical application with 0.5% DNCB and intradermal injection of PA 1mM
DNCB + 30mM PA	1% DNCB sensitization topical application with 0.5% DNCB and intradermal injection of PA 30mM

Figure 4. Experimental designs for modeling 2,4-dinitrochlorobenzene (DNCB)-induced dermatitis and summarized results from the measurement of their scratches.

(a) Mice received 200 μl of an acetone-ethanol mixture (3:1) including 1% DNCB in the nape of their necks for three days and then the same amount of an acetone : olive oil mixture (2:3) including 0.5% DNCB for 2 weeks. PA of different doses or 50 μl of the relevant vehicles were intradermally treated into the nape at the same time when 0.5% DNCB was treated. **(b)** PA treatment inhibited the spontaneous scratching behaviors of mice of *(a)*. Durations for scratching bouts were recorded for 1 h at the days listed (n = 7 per group). Data were analyzed by two-way ANOVA.

This article is protected by copyright. All rights reserved.

14765381, ja, Downloaded from https://bpspubs.onlinelibrary.wiley.com/doi/10.1111/bph.16201 by Gachon University Medical, Wiley Online Library on [06/08/2023]. See the Terms and Conditions (https://onlinelibrary.wiley.com/terms-and-conditions) on Wiley Online Library for rules of use; OA articles are governed by the applicable Creative Commons License

Figure 5

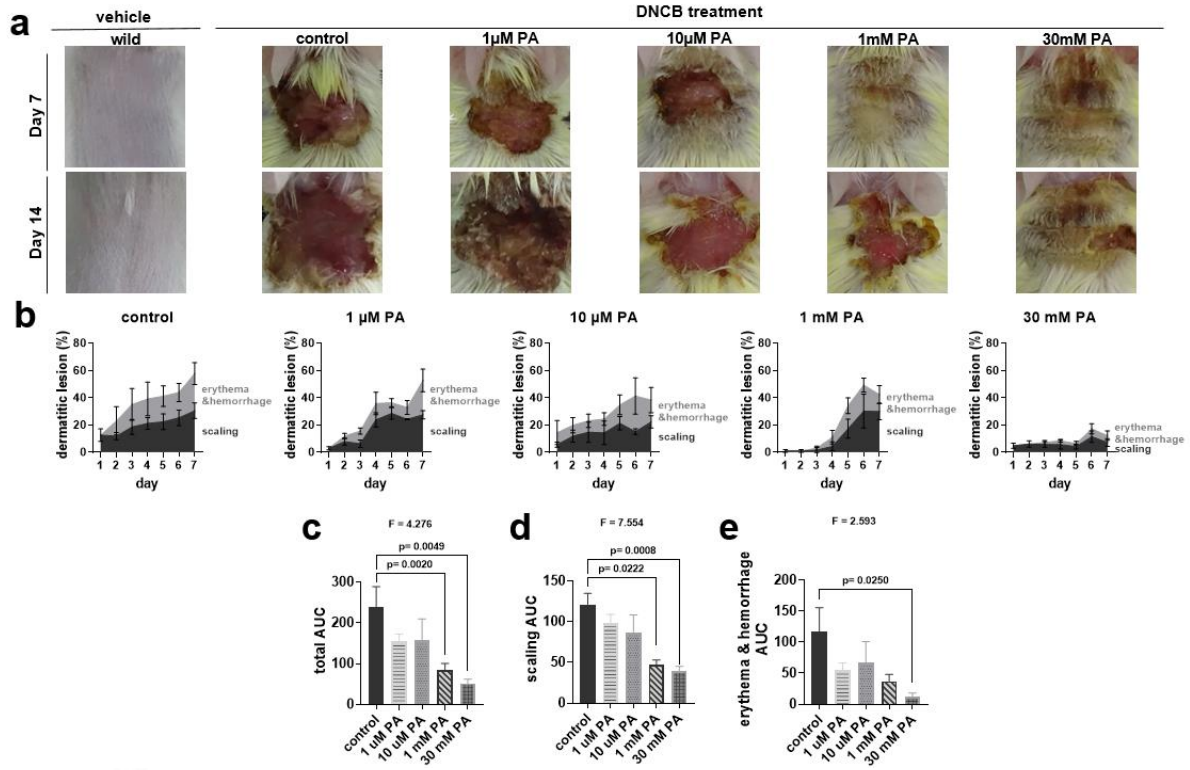

Figure 5. PA treatment dampened the lesions in mice with DNCB-induced dermatitis.

(a) Representative photographs of dorsal skin lesions of mice with or without PA treatment on day 7 and day 14 in the model indicated in figure 3(a). **(b)** Scaling (black area) and erythma and hemorrhage (grey area) were scored by quantifying the size ratios of the lesions indicating those symptoms to the shaved zones treated with each dose of DNCB.

(c) Area under the curves (AUCs) of the sum of black and grey areas with each dose of DNCB presented in *(b)* were compared using one-way ANOVA. **(d)** AUCs of the black areas (scaling) with each dose of DNCB presented in *(b)* were compared using one-way ANOVA.

(e) AUCs of the grey areas (erythma and hemorrhage) with each dose of DNCB presented in *(b)* were compared using one-way ANOVA.

This article is protected by copyright. All rights reserved.

14765381, ja, Downloaded from https://bpspubs.onlinelibrary.wiley.com/doi/10.1111/bph.16201 by Gachon University Medical, Wiley Online Library on [06/08/2023]. See the Terms and Conditions (https://onlinelibrary.wiley.com/terms-and-conditions) on Wiley Online Library for rules of use; OA articles are governed by the applicable Creative Commons License

Figure 6

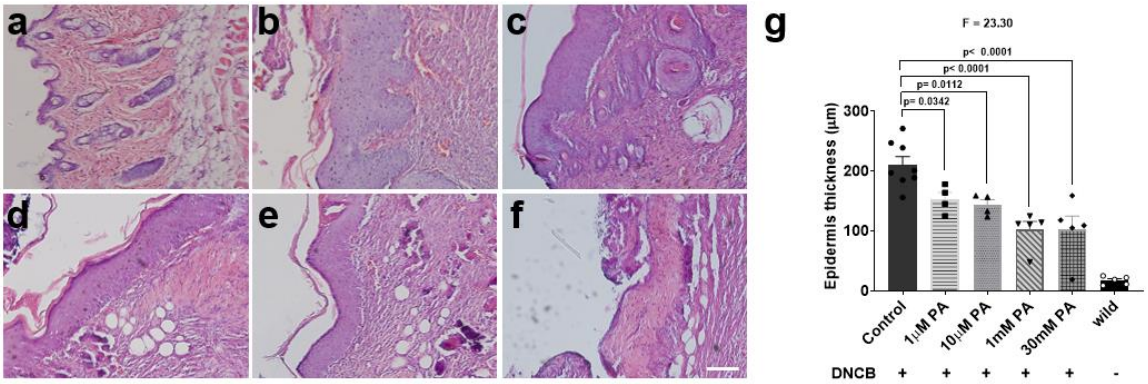

Figure 6. PA treatment disturbed epidermal thickening in mice with DNCB-induced dermatitis.

(a-f). Hematoxylin and eosin (H&E) staining of the sections of lesioned dorsal skin from groups of DNCB-treated mice on day 14 (scale bar, 100 μm). Representative results from mice without DNCB or PA treatment *(a)*, the control mice with DNCB and vehicle treatment *(b)*, mice treated with DNCB and 1 μM PA *(c)*, mice treated with DNCB and 10 μM PA *(d)*, mice treated with DNCB and 1 mM PA *(e)*, and mice treated with DNCB and 30 mM PA *(f)* were presented. The summary of quantifications and statistical comparison (one-way ANOVA) of the epidermal thickness measured from each mouse.

This article is protected by copyright. All rights reserved.

14765381, ja, Downloaded from https://bpspubs.onlinelibrary.wiley.com/doi/10.1111/bph.16201 by Gachon University Medical, Wiley Online Library on [06/08/2023]. See the Terms and Conditions (https://onlinelibrary.wiley.com/terms-and-conditions) on Wiley Online Library for rules of use; OA articles are governed by the applicable Creative Commons License

Pamoic Acid-Induced Peripheral GPR35 Activation Improves Pruritus and Dermatitis

Authors

Chaeeun Kim, Yerin Kim, Ji Yeon Lim, Minseok Kim, Haiyan Zheng, Miri Kim, Sun Wook Hwang*

KEY FINDING

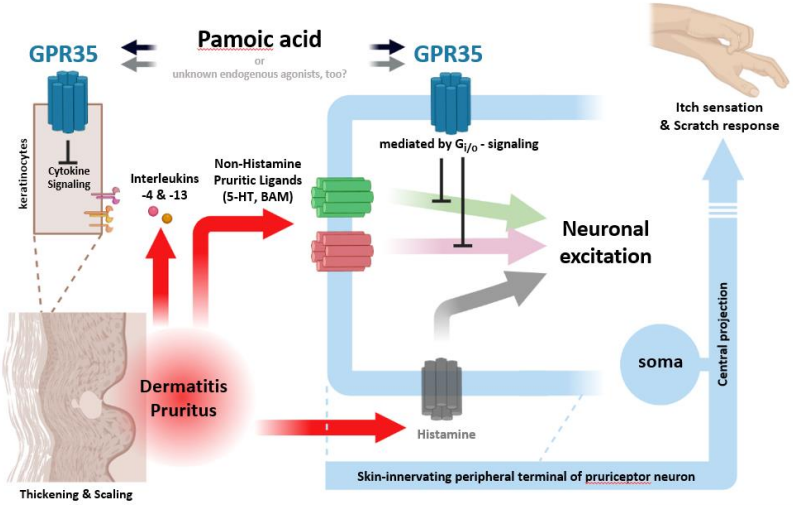

Kim, et al. *Br. J. Pharmacol.*
Graphical abstract was created with BioRender.com.

This article is protected by copyright. All rights reserved.

14765381, ja, Downloaded from https://bpspubs.onlinelibrary.wiley.com/doi/10.1111/bph.16201 by Gachon University Medical, Wiley Online Library on [06/08/2023]. See the Terms and Conditions (https://onlinelibrary.wiley.com/terms-and-conditions) on Wiley Online Library for rules of use; OA articles are governed by the applicable Creative Commons License